Technical University of Denmark

DTU

Effect of processing on fracture of binderfree all-cellulose composites

Goutianos, Stergios; Arevalo, R.; Sørensen, Bent F.; Peijs, T.

[Link to publication](#)

EFFECT OF PROCESSING ON FRACTURE OF BINDERFREE
ALL-CELLULOSE COMPOSITES

S. Goutianos[1], R. Arévalo[2], B.F. Sørensen[1] and T. Peijs[2]

[1]Department of Wind Energy, Section of Composites and Materials
Mechanics, Technical University of Denmark, Risø Campus, DK-
4000 Roskilde, Denmark
[2]Queen Mary, University of London, Centre of Materials Research,
School of Engineering and Materials Science, Mile End Road, E1 4NS
London, UK

ABSTRACT

Binderfree all-cellulose composites were prepared by a mechanical refinement process that allows the formation of intramolecular hydrogen bonds between the cellulose molecules during the drying process. The extent of this hydrogen bond network strongly depends on the duration of the refinement process. The fracture properties are studied at five different refining times. Due to the non-linear mechanical response of the binderfree all-cellulose composites, a method is first developed to obtain the fracture properties (fracture resistance and mode I cohesive law). The method uses a Double Cantilever Beam (DCB) sandwich specimen loaded with pure bending moments and it is based on the J integral. It is found that an increase of the refining times results a) in an increase of the crack initiation fracture energy and in a decrease of the steady-state fracture energy, and b) in an increase of the mode I peak cohesive traction.

1. INTRODUCTION

Natural fibre reinforced composites are attractive due to environmental and economical reasons. Thus, extensive research has been carried out over the last decades to improve their mechanical properties (Heijenrath and Peijs 1996; Van de Weyenberg, Ivens, De Coster, Kino, Baetens and Verpoest 2003). The attractiveness of natural fibres as an alternative reinforcement comes from their relatively high specific properties (Singleton, Baillie, Beaumont and Peijs 2005) and their eco-friendly performance when compared to traditional fibres such as glass fibres (Bos and Donald 1999).

Since natural fibres are based on renewable resources, the eco-performance of natural fibre composites is mainly controlled by the polymer matrix (Shen and Patel 2008). In waste management, one of the most favourite end-of-life options is recycling, which is limited in

233

natural fibre composites even if recyclable polymers such as polypropylene are used (Peijs 2003). If natural fibres are combined with a biodegradable matrix, such as polyhydroxybutyrate (PHB), polylactic acid (PLA) and starch, an additional disposal option becomes available through composting.

To address the environmental impact of the polymer matrix, self-reinforced fully recyclable cellulose composites, in which both the fibre and the matrix are composed of the same material have been developed in recent years (Nishino, Matsuda, and Hirao 2004; Gindl and Keckes 2005; Soykeabkaew, Nishino and Peijs 2009). These developments were based on the concept of all-polymer composites such as all-polypropylene composites (Ward and Hine 1997; Cabrera, Alcock, Loos and Peijs 2004). In all-polymer composites, both the fibre and the matrix are chemically identical resulting in excellent interfacial compatibility. Moreover, as these are mono-materials, fully recyclable and environmentally friendly materials with good mechanical properties can be obtained.

Two different approaches have been developed to manufacture all-cellulose composites: a) conventional impregnation methods of cellulose matrix into cellulose fibres (Nishino, Matsuda, and Hirao 2004; Grunert and Winter 2002) and b) selective dissolution methods where the skin of cellulose fibre is partially dissolved to form the matrix phase that bonds the fibres together (Nishino and Arimoto 2007). However, in both approaches, non-environmentally friendly solvents are used.

An alternative approach to create strong all-cellulose materials is to explore the potential of intramolecular bonding between cellulose molecules as in paper materials. In these processes the intrinsic bonding capability between cellulose fibres is used to enhance the Van der Waals or hydrogen bonded network. The key aspect to obtain materials with high mechanical properties is to increase the intramolecular-bonding network, which is achieved by increasing the specific-surface area of the fibres. A promising way to increase the cellulose network density is through the use of nanocelluloses (Berglund and Peijs 2010). However, nanofibres are often very costly. Thus, a different method was developed by Zellform GmbH, which involves the mechanical refinement of raw cellulose material (such as plant fibers or waste paper) into a sub-microfiber pulp having an increased degree of intramolecular bonding between the fibrils, which after drying and compaction in a hot-press results in a binderfree all-cellulose composite.

The mechanical properties of these composite products were found to outperform many conventional natural fibre composites in terms of stiffness and strength. These mechanical properties were found to increase with increasing the fibre refinement, due to the increase in network density (Arévalo, Achilli and Peijs 2013). In the present work, the fracture properties of these materials are examined as a function of the refinement time. The focus is to a) measure the fracture resistance / cohesive laws and b) observe the failure mechanisms during crack growth. Crack growth in cellulose networks can be complicated by the occurrence of crack bridging during crack growth and it resembles the fracture of paper (Isaksson and Hägglund 2007).

Such a toughening mechanism gives rise to fracture resistance with crack extension (R-curve behaviour) (Suo, Bao and Fan 1992) and therefore the fracture of these materials should not in general be characterised in terms of Linear Elastic Fracture Mechanics (LEFM). Instead, the fracture process zone can be modeled by non-linear fracture mechanics. The analysis followed is based on the J integral approach (Rice 1968) and a Double Cantilever Beam (DCB) sandwich specimen loaded with pure bending moments is used. Usually, in fracture mechanics analysis, the material outside the fracture process zone is assumed to be elastic. However, all-cellulose composites have a non-linear response and therefore it is necessary to take account of this non-linearity when calculating the fracture resistance. Thus, a general J integral based testing

approach, inspired by the work of Thouless, Kafkalidis, Ward and Bankowski (1997) who used the I integral, is first developed to obtain fracture resistance from the DCB experiments. It should be noted that the use of the J integral for materials having non-linear stress-strain relationship is allowed as long as there is no unloading of any material point so that the non-linear stress-strain behaviour can be considered as being a non-linear elastic material.

2. BASIC MECHANICS

The fracture properties are determined by the use of the DCB sandwich specimen shown in Fig. 1. It consists of the all-cellulose composite glued inside the grooves of two steel beams that are mounted on a special fixture (described in Section 3), which applies pure bending moments (Sørensen, Horsewell, Jøgensen, Kumar and Engbæk 1998). The fracture resistance can be calculated by evaluating the path independent J integral along a path over the external boundaries of the specimen.
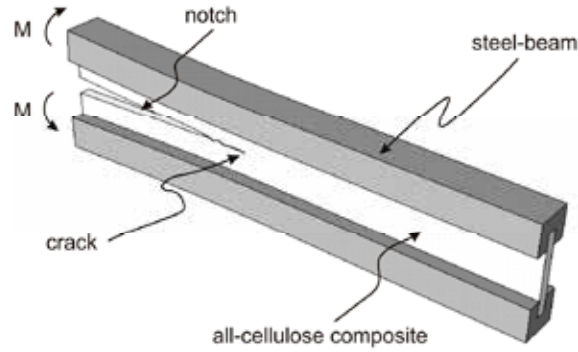

Fig. 1. Double Cantilever Beam (DCB) sandwich specimen loaded with pure bending moments.

To evaluate the two dimensional J integral, the non-uniform cross-section of the specimen (Fig.1) has to be transformed to an approximate equivalent cross-section of uniform width, B (the width of the steel beams). This can be achieved if the Young's modulus of the all-cellulose composite, E_2, is modified according to (Goutianos, Arévalo, Sørensen and Peijs 2013):

$$E_2^* = \eta\left(1 + I_o + \frac{I_o}{\Sigma}\right)E_2 \tag{1}$$

where $\Sigma = E_2/E_1$ with E_1 the Young's modulus of the steel beams, $\eta = b/B$ with b the width of the all-cellulose composite, and I_o a non-dimensional constant given by:

$$I_o = \frac{\rho - \rho^2 + \rho^3/3 - 2\rho\Delta + \rho^2\Delta + \rho\Delta^2}{\xi^3/3 + \xi^2 + \xi - \xi\Delta^2 - 2\xi\Delta + \xi\Delta^2} \tag{2}$$

where $\xi = h/H$ with $2h$ the height of the all-cellulose composite and H the height of the steel beam, $\rho = t/H$ with t the depth of the groove (Fig. 1), and Δ the normalised position of the neutral axis.

The modified cross-section allows an evaluation by the two dimensional J integral along a path along the external boundaries of the specimen as shown in Fig. 2.
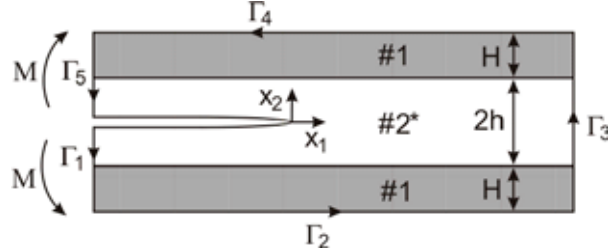

Fig. 2. Two-dimensional specimen representation and J integral path along the external boundaries.

The uni-axial tensile behaviour of the all-cellulose composites was found to be described by (Goutianos et al. 2013):

$$\sigma_{11} = \alpha_1 \varepsilon_{11} + \alpha_2 \varepsilon_{11}^2 \tag{3}$$

where α_1 is approximately equal to the Young's modulus of the all-cellulose composite. Eq. 3 is scaled according to Eq. 1. Then, the J integral solution for the sandwich specimen of Fig. 2 is given by (Goutianos et al. 2013):

$$J = -\frac{E_1 \widehat{\varepsilon}^2}{\eta \Delta^2}\left(-\Delta^2 H + \Delta H^2 - \frac{H^3}{3} \right) - \frac{\alpha_1 \widehat{\varepsilon}^2}{\eta \Delta^2}\left(-\frac{h^3}{3} - h^2(\Delta - H - h) - h(\Delta - H - h)^2 \right) -$$

$$-\frac{4\alpha_2 \widehat{\varepsilon}^3}{3\eta \Delta^3}\left(-\frac{h^4}{4} - h^3(\Delta - H - h) - \frac{3h^2}{2}(\Delta - H - h)^2 - h(\Delta - H - h)^3 \right) \tag{4}$$

where $\widehat{\varepsilon}$ is a function of the applied moment M. Since the J integral I is path independent, the local J integral surrounding the fracture process zone is equal to the J integral from Eq. 4, and thus the mode I cohesive law is given by (Sørensen and Jacobsen 2009):

$$\sigma = \frac{dJ_{loc}}{d\delta^*} \tag{5}$$

3. EXPERIMENTAL

3.1 Materials and Processing. The binderfree all-cellulose composites were based on flax fibres, with the process described in detail in Arévalo et al. (2013). The process involves a refining treatment stage where the flax fibres are cut and fibrillated in a highly dilute water suspension (2% cellulose). This suspension was subsequently filtered and dewatered to partially remove the water and to obtain the desired consistency for the subsequent compaction and drying steps. This fibre pulp was subjected to a room temperature pressing operation (10 bar) where further removal of water took place (~50% water content). This precursor was then finally dried in a hot-press where the application of pressure (40-80 bar) in combination with moderate heat (140°C) allowed the complete removal of all retained water, leading to well compacted flat

panels. An increase in refining time results in all-cellulose composites with improved mechanical properties in terms of Young's modulus and strength. In the present work, 5 different refining times were chosen. Representative SEM microgrpahs of the prepared specimens (before fracture) are shown in Fig. 3. An increase of the refining time results in an increased fibre fibrillation e.g. the number of fibrils increases and their size (length and cross section) decreases.
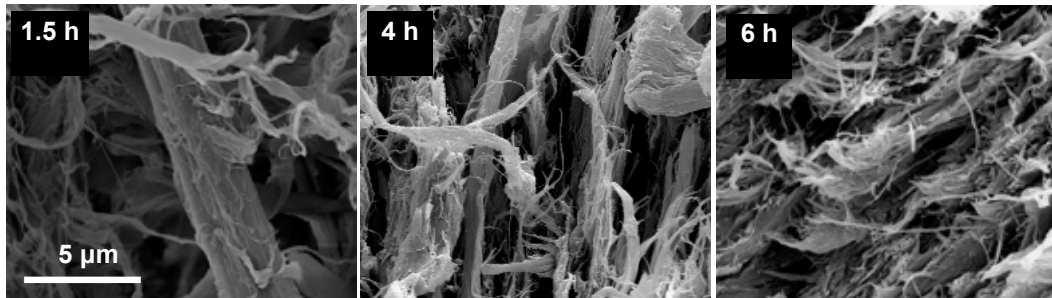

Fig. 3. SEM micrographs of the binderfree all-cellulose composites with a refining time of 1.5h, 4h, and 6h, respectively.

3.2 Specimen geometry. Rectangular specimens with a central notch along the biggest dimension were cut from all cellulose composite plates at dimensions approximately 10 mm x 65 mm x b mm. The width b varied from 1.2 to 2 mm depending on the refining time. The notch length (Fig. 1) was 25 mm and the height was approximately 1 mm. Further, a sharp crack was sawed manually at the root of the notch with a root radius less than 1.5 μm. The all-cellulose composite were then placed inside the grooves of two steel beams and glued using a two-part epoxy adhesive (Scotch-WeldTM DP460 from 3M).

3.3 Loading arrangement and instrumentation. The pure bending moments are applied to the DCB specimen using a special fixture (Sørensen et al. 1998), which can be operated inside the chamber of an environmental scanning electron microscope (ESEM) for in situ observation of the crack growth. In an ESEM the specimens need not be coated with conductive layers as in a conventional SEM where the new surfaces created by crack growth "charge up" and cannot be observed in detail. All the tests were conducted at room temperature and at a vapour pressure of 50 Pa. The fixture was mounted on the XY Z stage of the microscope (Zeiss Evo 60 EP-SEM) and thus by translating the stage in the specimen plane (XY) the crack growth increments could be measured.

3.4 Loading procedure. The DCB specimens were subjected to a monotonically increasing loading inside the ESEM. Images of the initial crack tip were recorded at different applied moments. As the moment increases, the end-opening of the crack tip increases. These openings represent the opening of the crack tip fracture process zone. At a certain moment, crack growth takes place. The moment was further increased and the images were recorded to measure the end-opening. These openings describe the bridging zone. The loading was stopped, when the steady-state fracture resistance was reached.

4.   RESULTS

Representative fracture resistance curves as a function of the end-opening are shown in Fig. 4. The fracture resistance increases from a relatively low value, corresponding to failure process

zone at the crack tip, to a steady-state level, as the bridging zone evolves. The fracture resistance steady-state value decreases with increasing the refining time. The end-opening at which the steady-state is attained is almost independent of the refining time. The initial slope of the fracture resistance curves, up to end-openings less than 5 μm, describe the crack tip fracture process zone. The steeper slope is observed for a refining time of 6h and decreases with decreasing the refining time. The enhanced fibrillation at 6h results in a more extensive hydrogen-bonded network between the fibrils. Such a strong network structure would result in a higher fracture resistance for crack initiation (steeper initial slope in Fig. 4). For end-openings larger than approximately 5 μm, the fracture resistance curves describe the bridging failure mechanism which is controlled by the length of the fibres and the adhesion between them, i.e. short fibres (6h refining time) are less effective in bridging the crack faces and therefore the increase in fracture resistance is less pronounced.
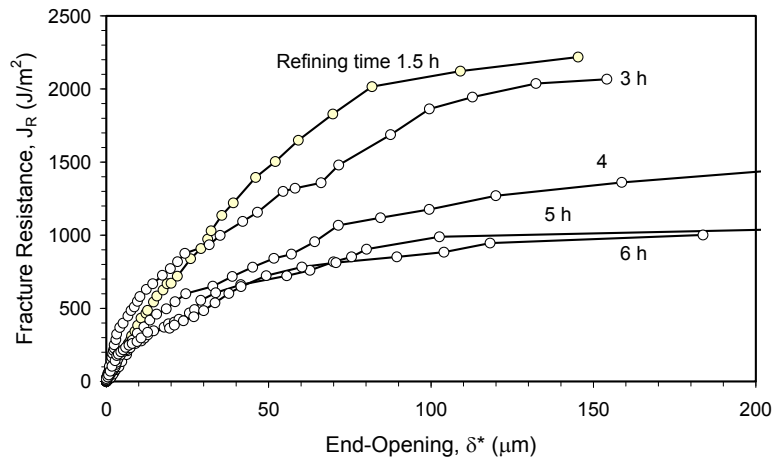

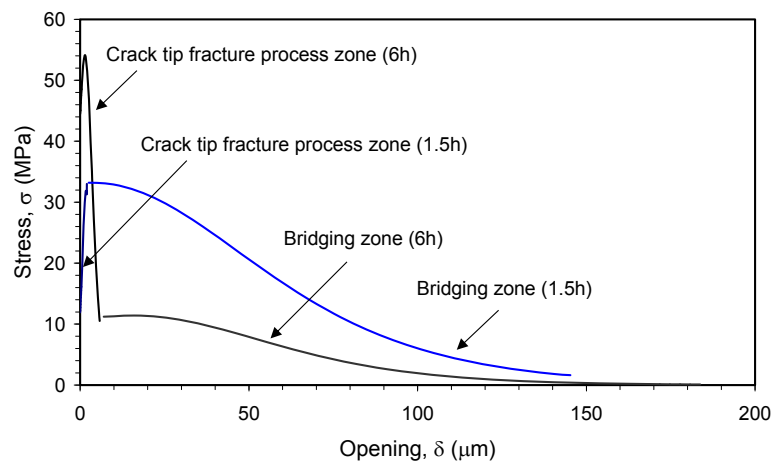Fig. 4. Effect of the refining time on the fracture resistance, J_R.

Fig. 5. Examples of cohesive laws for refining times 1.5h and 6h, respectively.

In order to obtain the cohesive laws from the fracture resistance curves of Fig. 4, the experimental data are first fitted with a non-linear function and the differentiated with respect to the end-opening (Goutianos et al. 2013). For each curve the experimental data are split in two parts. The fist part corresponds to the opening of the crack tip fracture process zone, and the second part to the bridging zone. The transition point is determined from observations during the in-situ experiments. The representative cohesive laws for 1.5h and 6h are given in Fig. 5. The peak cohesive stress is significantly higher for 6h refining time than 1.5h. However, the traction in the bridging zone is higher for the shorter refining time (1.5h).

Fig. 6 shows as an example of the observations made by performing the experiments inside the chamber of the ESEM. In Fig. 6 extensive fibre bridging can be seen for binderfree all-cellulose composites with a refining time of 1.5h because the flax fibres are larger in size (length and diameter). Such large fibres can effectively bridge the crack faces even for large crack openings. This can explain the higher steady-state fracture resistance (see Fig. 4) and higher cohesive tractions in the bridging zone (Fig. 5).
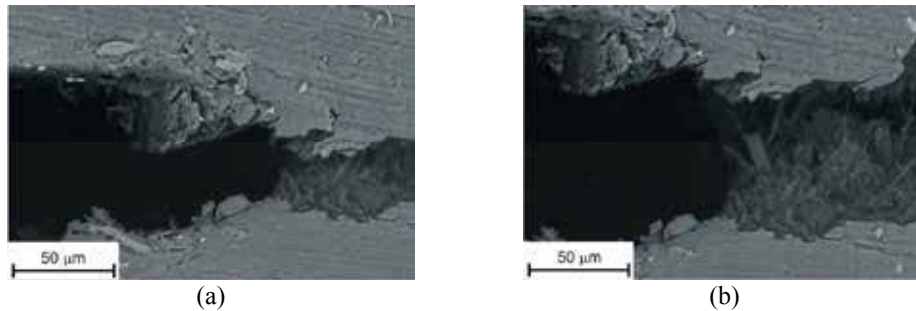

| (a) | (b) |

Fig. 6. Backscatter electron micrographs showing the end-opening of the fracture process zone at increasing applied moment for 1.5 h refining treatment.

5.   CONCLUSIONS

The fracture properties of binderfree all-cellulose composites with different levels of fibre fibrillation were studied. A general J integral based method for mode I fracture mechanics characterisation taking account of the non-linear response of the all-cellulose composites was developed using DCB sandwich specimens loaded with pure bending moments. The experiments were performed inside an environmental scanning electron microscope to observe the failure mechanisms, determine the crack initiation, and measure the crack length. It was found that:
   a) The fracture resistance for crack initiation and peak cohesive stress both increase with increasing fibre fibrillation. This is due to the presence of a stronger Van der Waals or hydrogen bonded network structure in all-cellulose composites with higher refining time.
   b) The steady-state fracture resistance decreases with increasing fibre fibrillation. An increase in refining time results not only in a reduction in fibre diameter but also in shorter fibres and thus in a lower fracture resistance with increasing refining times.

Council for Strategic Research.

REFERENCES

Arévalo, R., Achilli, L, and Peijs, T. (2013). Binderfree all-cellulose composites. In preparation.

Berglund, L. A. and Peijs, T. (2010). Cellulose biocomposites - from bulk moldings to nanostructured systems. MRS Bulletin 35, 201–207.

Bos, H. L. and Donald, A. M. (1999). In situ ESEM study of the deformation of elementary flax fibres. Journals of Materials Science 34, 3029-3034.

Cabrera, N., Alcock, B., Loos, J., and Peijs, T. (2004). Processing of all-polypropylene composites for ultimate recyclability, Proceedings of the Institution of Mechanical Engineers, Part L: Journal of Materials: Design and Applications 218, 145–155.

Gindl, W., and Keckes, J. (2005). All-cellulose nanocomposite, Polymer 46, 10221–10225.

Goutianos, S., Arévalo, R., Sørensen, B. F., and Peijs, T. (2013) Effect of processing conditions on fracture resistance and cohesive Laws of binderfree all-cellulose composites. In preparation.

Grunert, M. and Winter, W. T. (2002). Nanocomposites of cellulose acetate butyrate reinforced with cellulose nanocrystals, Journal of Polymers and the Environment 10, 27–30.

Heijenrath, R. and Peijs, T. (1996). Natural-fibre-mat-reinforced thermoplastic composites based on flax fibres and polypropylene. Advanced Composites Letters 5, 81-85.

Isaksson, P., and Hägglund, R. (2007). Evolution of bond fractures in a randomly distributed fiber network. International Journal of Solids and Structure 44, 6135–6147.

Nishino, T., Matsuda, I., and Hirao, K. (2004). All-cellulose composite. Macromolecules 37, 7683–7687.

Nishino, T. and Arimoto, N. (2007). All-cellulose composite prepared by selective dissolving of fiber surface. Biomacromolecules 8, 2712–2716.

Peijs, T. (2003). Composites for recyclability. Materials Today 6, 30-35.

Rice, J. R. (1968). A path independent integral and the approximate analysis of strain concentrations by notches and cracks, Journal of Applied Mechanics 35, 379–386.

Shen, L., and Patel, M. K. (2008). Life cycle assessment of polysaccharite materials: A review. Journal of Polymers and the Environment 16, 154–167.

Singleton, A. C. N., Baillie, C. A., Beaumont, P. W. R. and Peijs, T. (2005). On the mechanical properties, deformation and fracture of a natural fibre/recycled polymer composite. Composites Part B: Engineering 36, 245-255.

Soykeabkaew, N., Nishino, T., and Peijs, T. (2009). All-cellulose composites of regeneratedcellulose fibres by surface selective dissolution, Composites Part A: Applied Science and Manufacturing 40, 321–328.

Suo, Z., Bao, G., and Fan, B. (1992). Delamination R-curve phenomena due to damage. Journal of the Mechanics and Physics of Solids 40, 1–16.

Sørensen, B. F., Horsewell, A., Jøgensen, O., Kumar, A. N., Engbæk, P. (1998). Fracture resistance measurement method for in situ observation of crack mechanisms, Journal of the American Ceramic Society 81, 661–669.

Sørensen, B .F., and Jacobsen, T. K. (2009). Characterizing delamination of fibre composites by mixed mode cohesive laws. Composites Science and Technology 69, 445-456.

Thouless, M., Kafkalidis, M., Ward, S., and Bankowski, Y. (1997). Toughness of plastically-deforming asymmetric joints, Scripta Materialia 37, 1081–1087.

Van de Weyenberg, I., Ivens, J., De Coster, A., Kino, B., Baetens, E., and Verpoest, I. (2003). Influence of processing and chemical treatment of flax fibres on their composites. Composites Science and Technology 63, 1241-1246.

Ward, I. M. and Hine, P. J. (1997). Novel composites by hot compaction of fibers. Polymer Engineering & Science 37, 1809–1814.